Maximal planar networks with large clustering coefficient and power-law degree distribution

Tao Zhou,[1,2] Gang Yan,[2] and Bing-Hong Wang[1,*]
[1]*Nonlinear Science Center and Department of Modern Physics, University of Science and Technology of China, Hefei Anhui, 230026, People's Republic of China*
[2]*Department of Electronic Science and Technology, University of Science and Technology of China, Hefei Anhui, 230026, People's Republic of China*
(Received 30 September 2004; revised manuscript received 21 December 2004; published 28 April 2005)

In this article, we propose a simple rule that generates scale-free networks with very large clustering coefficient and very small average distance. These networks are called **random Apollonian networks** (RANs) as they can be considered as a variation of Apollonian networks. We obtain the analytic results of power-law exponent $\gamma=3$ and clustering coefficient $C=\frac{46}{3}-36\ln\frac{3}{2}\approx 0.74$, which agree with the simulation results very well. We prove that the increasing tendency of average distance of RANs is a little slower than the logarithm of the number of nodes in RANs. Since most real-life networks are both scale-free and small-world networks, RANs may perform well in mimicking the reality. The RANs possess hierarchical structure as $C(k)\sim k^{-1}$ that are in accord with the observations of many real-life networks. In addition, we prove that RANs are maximal planar networks, which are of particular practicability for layout of printed circuits and so on. The percolation and epidemic spreading process are also studied and the comparisons between RANs and Barabási-Albert (BA) as well as Newman-Watts (NW) networks are shown. We find that, when the network order N (the total number of nodes) is relatively small (as $N\sim 10^4$), the performance of RANs under intentional attack is not sensitive to N, while that of BA networks is much affected by N. And the diseases spread slower in RANs than BA networks in the early stage of the suseptible-infected process, indicating that the large clustering coefficient may slow the spreading velocity, especially in the outbreaks.

DOI: 10.1103/PhysRevE.71.046141 PACS number(s): 89.75.Hc, 64.60.Ak, 84.35.+i, 05.40.−a

I. INTRODUCTION

Many social, biological, and communication systems can be properly described as complex networks with nodes representing individuals or organizations and edges mimicking the interactions among them [1–14]. Examples are numerous: these include the Internet [15–17], the World Wide Web [18–22], social networks of acquaintance or other relations between individuals [23–34], metabolic networks [35–39], food webs [40–46], and many others [47–58]. The ubiquity of complex networks inspires scientists to construct a general model. In the past 200 years, the study of topological structures of the networks used to model the interconnection systems has gone through three stages. For over a century, there was an implicit assumption that the interaction patterns among the individuals can be embedded onto a regular structure such as Euclidean lattices, hypercube networks, and so on [59–62]. Since late 1950s mathematicians began to use random graphs to describe the interconnections, this is the second stage [63–70]. In the past few years, with the computerization of data acquisition process and the availability of high computing powers, scientists have found that most real-life networks are neither completely regular nor completely random. The results of many empirical studies and statistical analyses indicate that the networks in various fields have some common characteristics, the most important of which are called small-world effect [71–76] and scale-free property [77–80].

In a network, the distance between two nodes is defined as the number of edges along the shortest path connecting them. The average distance L of the network, then, is defined as the mean distance between two nodes, averaged over all pairs of nodes. The average distance is one of the most important parameters to measure the efficiency of communication networks. For instance, in a store-forward computer network, probably the most useful measurement of its performance is the transmission delay (or time delay) encountered by a message traveling through the network from its source to destination; this is approximately proportional to the number of edges a message must pass through. Thus the average distance plays a significant role in measuring the transmission delay. The number of edges incident from a node x is called the degree of x, denoted by $k(x)$. Obviously, through the $k(x)$ edges, there are $k(x)$ nodes that are correlated with x; these are called the neighbor set of x, and denoted by $A(x)$. The clustering coefficient $C(x)$ of node x is the ratio between the number of edges among $A(x)$ and the total possible number; the clustering coefficient C of the whole network is the average of $C(x)$ over all x. Empirical studies indicate that most real-life networks have much smaller average distance (as $L\sim\ln N$ where N is the number of nodes in the network) than the completely regular networks and much greater clustering coefficient than those of the completely random networks. Therefore they should not be treated as either completely regular or random networks. The recognition of small-world effect involves the two factors mentioned above: a network is called a small-world network as long as it has small average distance and great clustering coefficient. Another important characteristic in real-

*Electronic address: bhwang@ustc.edu.cn

life networks is the power-law degree distribution, that is $p(k) \propto k^{-\gamma}$, where k is the degree and $p(k)$ is the probability density function for the degree distribution. γ is called the power-law exponent, and is usually between 2 and 3 in real-life networks [1–3]. This power-law distribution falls off much more gradually than an exponential one, allowing for a few nodes of very large degree to exist. Networks with power-law degree distribution are referred to as scale-free networks, although one can and usually does have scales present in other network properties.

From 1998 much attention has been focused on how to model a complex network. One of the most well-known models is Watts and Strogatz's small-world network (WS network), which can be constructed by starting with a regular network and randomly moving one endpoint of each edge with probability p [72]. Another popular model was proposed independently by Monasson [75] and by Newman and Watts(NW networks) [74], where no edges are rewired. Some variations of the small-world model have been proposed. Several authors have studied the model in dimension higher than one and obtained similar results to the one dimension case [74,81–84]. Another kind of model in which shortcuts preferentially join nodes that are close together on the underlying lattice also have been studied [85–87]. Very recently, Zhu *et al.* proposed a so-called directed dynamical small-world model, in which the network structure is affected by the processes upon the network [76].

Another significant model is Barabási and Albert's scale-free network model (BA network) [77,78], which is very similar to Price's [79,80]. The BA model suggests that two main ingredients of self-organization of a network in a scale-free structure are growth and preferential attachment. These point to the facts that most networks grow continuously by adding new nodes, which are preferentially attached to existing nodes with a large number of neighbors. The subsequent researches on various processes taking place upon complex networks, such as percolation [83,88–99], epidemic processes [100–107], cascade processes [108–116], and so on, indicate that the scale-free degree distribution may play the most crucial role rather than small-world effect. Therefore, in the past 2 or 3 years, the study of modeling complex networks focuses on revealing the underlying mechanism of power-law degree distribution. Roughly, these models for scale-free networks can be classified into three main scenarios. The first one is related to the models of human behavior [117,118] and was introduced in a network version under the name "preferential attachment" mentioned above [77,78,119–131]. The second class of models is where a scale-free distribution appears as a result of a balance between a modeled tendency to form hubs against an entropic pressure towards a random network with an exponential degree distribution [132–134]. The third one is the self-organized models that lead to power-law degree distribution [135–141].

In the recent several months, a few authors have demonstrated the use of pure mathematical objects and methods to construct scale-free networks. One interesting instance is the so-called integer networks [142], in which the nodes represent integers and two nodes x and y are linked by an edge if and only if x is divided exactly by y or y is divided exactly by x, where x and y are nonzero integers. Zhou *et al.* have studied the statistical properties of these networks and demonstrated that they are scale-free networks of large clustering coefficient. Another significant instance is **Apollonian network** (ANs) introduced by Andrade *et al.* [143]. In our opinion, Apollonian networks may be not the networks of best performance, but assuredly the most beautiful ones we have ever seen. Another related work is owed to Dorogovtsev and Mendes *et al.*, in which the deterministic networks, named **pseudofractals**, are obtained by random attachment aiming at edges [144,145].

In this article, we propose a simple rule that generates scale-free networks with a very large clustering coefficient and very small average distance. These networks are called **random Apollonian networks** (RANs), since they can be considered as a variation of Apollonian networks [151]. We discuss the difference between RANs and ANs in detail(in addition, the difference between RANs and BA networks), and demonstrate that RANs perform much better than BA networks in some aspects.

This article is organized as follow: In Sec. II, the Apollonian networks are introduced. In Sec. III, the rule that generates RANs is described in detail. In Sec. IV, we give both the simulation and analytic results about the statistical characteristics of RANs, including the scale-free property and the small-world effect, where the detailed analytic processes are shown in the Appendixes. In Sec. V, we prove that RANs are the maximal planar networks. In Sec. VI, the percolation and epidemic spreading process are also studied and the comparisons between RANs and BA networks as well as NW networks are shown. Finally, we sum up this article and discuss the relevance of RANs to the real world in Sec. VII.

II. BRIEF INTRODUCTION OF APOLLONIAN NETWORKS

Apollonian networks, introduced by Andrade *et al.* [143], are derived from the problem of space-filling packing of spheres according to the ancient Greek mathematician Apollonius of Perga [146]. To produce an Apollonian packing, we start with an initial array of touching disks, the interstices of which are curvilinear triangles. In the first generation disks are added inside each interstice in the initial configuration, such that these disks touch each of the disks bounding the curvilinear triangles. The positions and radii of these disks can easily be calculated, and the circle size distribution follows a power law with an exponent of about 1.3 [146]. Of course, these added disks cannot fill 1all of the space in the interstices, but instead give rise to three smaller interstices. In the second generation, further disks are added inside all of these new interstices, which again touch the surrounding disks. This process is then repeated for successive generations. If we denote the number of generations by t, where $t=0$ corresponds to the initial configuration, as $t\to\infty$ the space-filling Apollonian packing is obtained as shown in Fig. 1. Apollonian packing can be used as a basis of a network, where each disk is a node in the network and nodes are connected if the corresponding disks are in contact. We call this contact an "Apollonian network." Figure 2 shows how

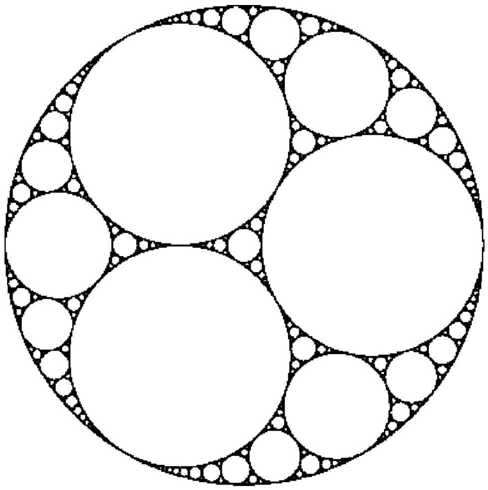

FIG. 1. An Apollonian packing of disks within a circle [147].

the network evolves with the addition of new nodes at each generation. For each new disk added, three new interstices in the packing are created, which will be filled in the next generation. Equivalently, for each new node added, three new triangles are created in the network, into which nodes will be inserted in the next generation.

Doye *et al.* have studied the properties of Apollonian networks in detail [147] and shown the degree distribution $p(k) \propto k^{-\gamma}$, average length $l \propto (\ln N)^{\beta}$, where $\gamma = 1 + (\ln 3/\ln 2) \approx 2.585$, $\beta \approx 0.75$ and N is the order [148] of the network; in other words, Apollonian networks are scale free and display small-world effect. It is worth remarking that the clustering coefficient C is close to 0.828, much larger than that of BA networks, in the limit of large N.

Andrade *et al.* have also found many peculiar results about some well-known models upon Apollonian networks, including percolation, electrical conduction, and a magnetic model [143,150].

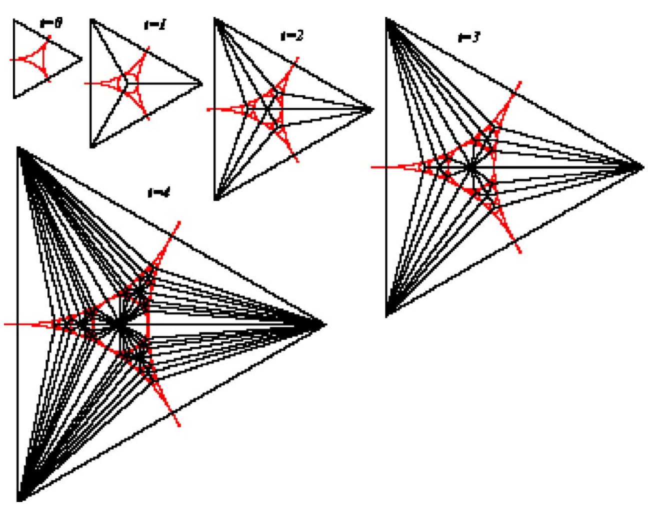

FIG. 2. (Color online) The development of the 2D Apollonian network inside the interstice between three mutually touching disks, as the number of generations increase. In each picture, the network is overlaid on the underlying packing [147].

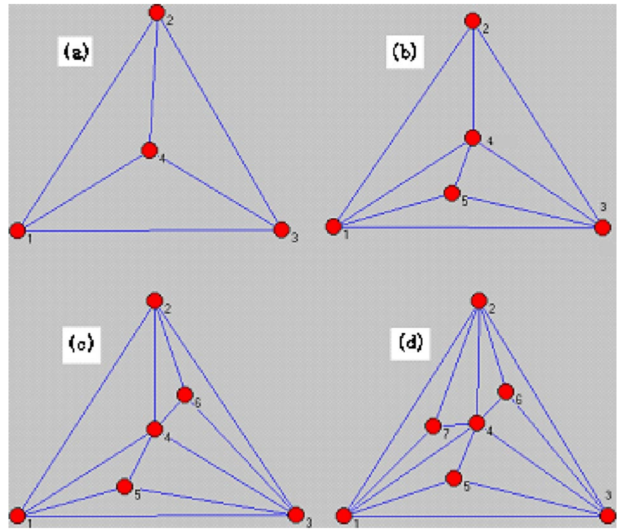

FIG. 3. (Color online) The sketch maps for the network growing process. The four figures show a possible growing process for RANs at time $t=1$ (a), $t=2$ (b), $t=3$ (c), and $t=4$ (d). At time step 1, the fourth node is added to the network and linked to nodes 1, 2, and 3. Then, at time step 2, the triangle $\Delta 134$ is selected, the fifth node is added inside this triangle and linked to nodes 1, 3, and 4. After that, the triangles $\Delta 234$ and $\Delta 124$ are selected at time steps 3 and 4, respectively. Nodes 6 and 7 are added inside these two triangles respectively. (d) shows a random Apollonian network of order 7. Keeping on the similar iterations, one can get RANs of any orders as he likes.

III. RANDOM APOLLONIAN NETWORKS

A random Apollonian network starts with a triangle containing three nodes marked as 1, 2, and 3. Then, at each time step, a triangle is randomly selected, and a new node is added inside the triangle and linked to the three vertices of this triangle. The sketch maps for the network growing process are shown in Fig. 3.

It is clear that, at time step t, our network is of order $N = t+3$. Using this simple rule, one can get the random Apollonian network of arbitrary order that he likes. Note that the randomicity is involved in our model(that is why we call these networks random Apollonian networks); the analytic approaches are completely different from the earlier studies on Apollonian networks.

IV. STATISTICAL CHARACTERISTICS OF RANDOM APOLLONIAN NETWORKS

A. The scale-free property

As we have mentioned above, the degree distribution is one of the most important statistical characteristics of networks. Since a majority of real-life networks are scale-free networks, whether the networks are of power-law degree distribution is a criterion to judge the validity of the model. In this subsection, we will give the simulation and analytic results on random Apollonian networks' degree distribution.

Note that, after a new node is added to the network, the number of triangles increases by 2 [152]. Therefore, we can immediately get that when the network is of order N, the number of triangles is

$$N_\Delta = 2(N-3) + 1 = 2N - 5. \tag{1}$$

Let N_Δ^i denote the number of triangles containing the ith node. The probability that a newly added node will link to the ith node is N_Δ^i/N_Δ. Apparently, except for the nodes 1, 2, and 3, N_Δ^i is equal to the degree of the ith node: $N_\Delta^i = k_i$. Therefore, we can write down a rate equation [119] for the degree distribution. Let $n(N,k)$ be the number of nodes with degree k when N nodes are present. Now we add a new node to the network; $n(N,k)$ evolves according to the following equation:

$$n(N+1,k+1) = n(N,k)\frac{k}{N_\Delta} + n(N,k+1)\left(1 - \frac{k+1}{N_\Delta}\right). \tag{2}$$

When N is sufficient large, $n(N,k)$ can be approximated as $Np(k)$, where $p(k)$ is the probability density function for the degree distribution. In terms of $p(k)$, the above equation can be rewritten as

$$(N+1)p(k+1) = \frac{Nkp(k)}{N_\Delta} + Np(k+1) - \frac{N(k+1)p(k+1)}{N_\Delta}. \tag{3}$$

Using Eq. (1) and the expression $p(k+1)-p(k)=dp/dk$, we can get the continuous form of Eq. (3):

$$k\frac{dp}{dk} + \frac{3N-5}{N}p(k) = 0. \tag{4}$$

This leads to $p(k) \propto k^{-\gamma}$ with $\gamma=(3N-5)/N \approx 3$ for large N.

In Fig. 4, we report the degree distribution for $N = 640\,000$, $320\,000$, $160\,000$, $80\,000$, $40\,000$, and $20\,000$. The simulation results agree very well with the analytic one.

By the way, some readers may think the RANs are almost the same as BA networks. Indeed, the two ingredients, "growth" and "preferential attachment," are in common and they have almost the same power-law exponent, but further simulation and analytic results will show that RANs and BA networks are essentially different in some aspects and RANs may be closer to reality than BA networks.

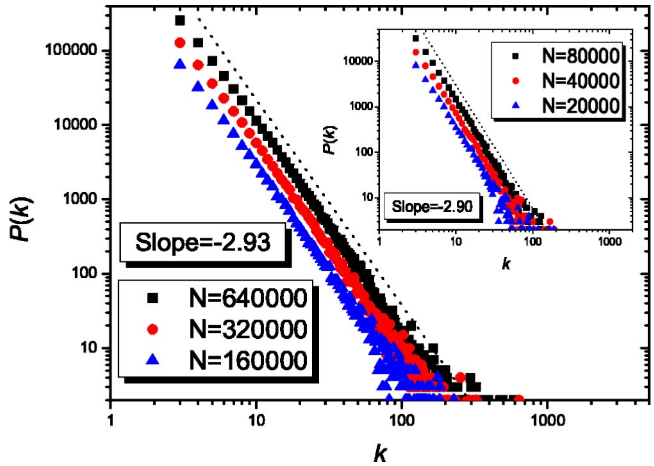

FIG. 4. (Color online) The degree distribution of RANs, with $N=640\,000$ (black squares), $N=320\,000$ (red circles), and $N=160\,000$ (blue triangles). In this figure, $P(k)$ denotes the number of nodes of degree k. The power-law exponents γ of the three probability density function are $\gamma_{640\,000}=2.94\pm0.04$, $\gamma_{320\,000}=2.92\pm0.05$, and $\gamma_{160\,000}=2.92\pm0.06$, respectively. The average exponent of them is 2.93. The inset shows degree distribution of RANs, with $N=80\,000$ (black squares), $N=40\,000$ (red circles), and $N=20\,000$ (blue triangles). The exponents are $\gamma_{640\,000}=2.91\pm0.07$, $\gamma_{320\,000}=2.90\pm0.07$, and $\gamma_{160\,000}=2.90\pm0.09$. The mean value is 2.90. The two dash lines have slope -3.0 for comparison.

B. The small-world effect

The small-world effect consists of two properties: a large clustering coefficient and small average distance. In this subsection, we will give both the simulation and analytic results about the two properties and prove that RANs are small-world networks.

At first, let us calculate the clustering coefficient of RANs. As we mentioned in Sec. I, for an arbitrary node x, the clustering coefficient $C(x)$ is

$$C(x) = \frac{2E(x)}{k(x)[k(x)-1]}, \tag{5}$$

where $E(x)$ is the number of edges among node x's neighbor set $A(x)$, and $k(x)=|A(x)|$ is the degree of node x. The clustering coefficient C of the whole network is defined as the average of $C(x)$ over all nodes.

By means of theoretic calculation(see Appendix A for details), we obtain the clustering coefficient of RANs with large order N as

$$C = \tfrac{46}{3} - 36\ln\tfrac{3}{2} \approx 0.74. \tag{6}$$

Figure 5 shows the simulation results about the clustering coefficient of RANs, which agree well with the analytic one. It is remarkable that the clustering coefficient of BA networks is very small and decreases with the increasing of network order, following approximately $C \sim \ln^2 N/N$ [149]. The simulation about the clustering coefficient of the BA network can also be seen in Fig. 5. Since the data-flow patterns show a large amount of clustering in interconnection networks, the RANs may perform better than BA networks. In addition, the demonstration exhibits that most real-life networks have a large clustering coefficient no matter how many nodes they have. That agrees with the case of RANs but conflicts with the case of BA networks, thus RANs may be more appropriate to mimic the reality.

In addition, many real-life networks including Internet, World Wide Web, and the actor network, are characterized by the existence of hierarchical structure [153–155], which can usually be detected by the negative correlation between the clustering coefficient and the degree. The BA network, which does not possess hierarchical structure, is known to have the clustering coefficient $C(x)$ of node x independent of its degree $k(x)$ [153], while the RAN has been shown to have $C(k) \sim k^{-1}$ [see Eq. (A2)], in accord with the observations of many real-life networks [153].

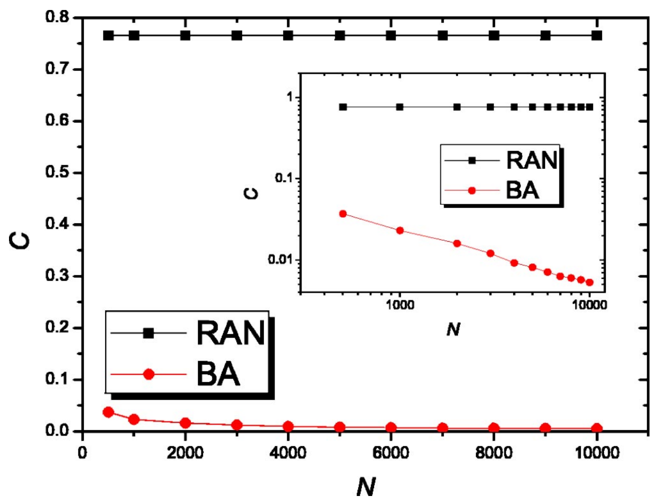

FIG. 5. (Color online) The clustering coefficient of RANs (black squares) and BA networks (red circles). In this figure, one can find that the clustering coefficient of RANs is almost a constant a little smaller than 0.77, which accords with the analytic very well. The dashed line represents the analytic result 0.74. It is clear that the clustering coefficient of BA networks is much smaller than that of RANs. The inset shows that the clustering coefficient of BA networks decreases with the increasing of network order quickly, which is quite different from the real-life networks. All the data are obtained by ten independent simulations.

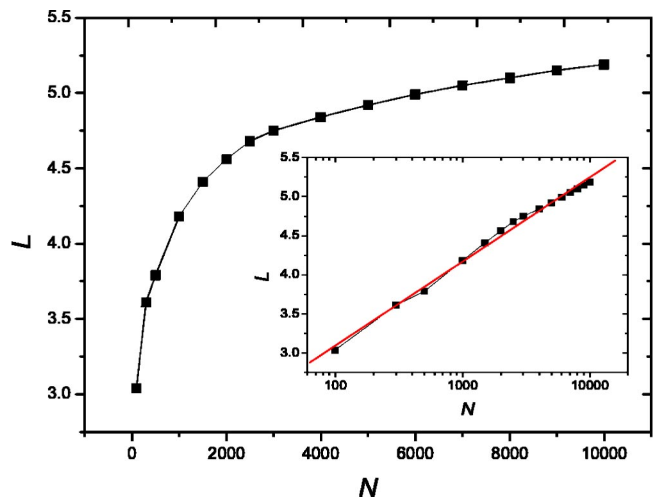

FIG. 6. (Color online) The dependence between the average distance L and the order N of RANs. One can see that L increases very slowly as N increases. The inset exhibits the curve where L is considered as a function of $\ln N$, which is well fitted by a straight line. The curve is above the fitting line when N is small $(1000 \leqslant N \leqslant 3000)$ and under the fitting line when N is large $(N \geqslant 4000)$, which indicates that the increasing tendency of L can be approximated as $\ln N$ and in fact a little slower than $\ln N$. All the data are obtained by ten independent simulations.

In succession, let us discuss the average distance of RANs. By means of theoretic approximate calculation (see Appendix B for details), we prove that the increasing tendency of $L(N)$ is a little slower than $\ln N$. In Fig. 6, we report the simulation results on the average distance of RANs, which agree well with the analytic result.

In respect that the random Apollonian networks are of very large clustering coefficient and very small average distance, they are not only the scale-free networks, but also small-world networks. Since many real-life networks are both scale-free and small-world networks, RANs may perform better in mimicking reality than WS and BA networks.

V. THE PLANARITY OF RANDOM APOLLONIAN NETWORKS

There are many practical situations in which it is important to decide whether a given network is planar, and, if so, to then find a planar embedding of the network. For example, a very large scale integrated (VLSI) designer has to place the cells on printed circuit boards according to several designing requirements. One of these requirements is to avoid crossings since they may lead to undesirable signals. One is, therefore, interested in knowing if a given electrical network is planar, where the nodes correspond to electrical cells and the edges to the conductor wires connecting the cells.

A network is a planar network if it can be drawn in the plane in such a way that no two edges intersect. Putting it a little more rigorously, it is possible to represent it by a drawing in the plane in which the nodes correspond to distinct points and the edges to simple Jordan curves connecting the points of its end points. In this drawing every two curves are either disjoint or meet only at a common end point. The above representation of a graph is said to be a plane network.

In some places, the networks will perform better when they have more edges. Therefore, how to add more edges into a network but keeping it a planar network is a practical and interesting problem. According to the rule that generates RANs, one can immediately find that RANs are planar networks. Hereinafter, we will show that the RANs are maximal planar networks, which are the planar networks with fixed order that have maximum edges.

If we omit the nodes and edges of a planar network from the plane, the remainder falls into connected components, called faces [62]. Clearly, each plane network has exactly one unbounded face and each edge is in the boundary of two faces. If we draw the graph of a convex polyhedron in the plane, then the faces of the polyhedron clearly correspond to the faces of the plane networks. This leads to the Euler's polyhedron theorem or simply Euler's formula [60–62] that if a connected plane network has n nodes, m edges, and f faces, then

$$n - m + f = 2. \tag{7}$$

Furthermore, denote f_i as the number of faces having exactly i edges in their boundaries. Clearly,

$$\sum_i f_i = f. \tag{8}$$

And since each edge is in the boundary of two faces, we have

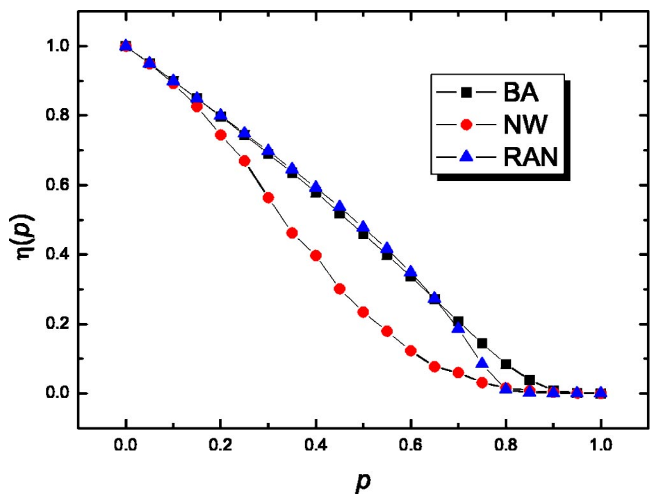

FIG. 7. (Color online) The random site-percolation transition for RANs (blue triangles), and NW (red circles) and BA (black squares) networks. Plotted is the fraction of nodes that remains in the giant component after random breakdown of a fraction p of all nodes, $\eta(p)$, as a function of p. All the networks used for numerical study are of order $N=10\,000$ and $\langle k\rangle=6$. Clearly, the scale-free networks (BA and RAN) are much more resilient than networks of single scale (NW), which agrees with the well-known conclusion [88,91]. When $p<0.3$, the performances of RANs and BA networks under random failures are almost the same; when $0.3<p<0.6$, RANs are a little more resilient than BA networks; when p becomes even larger, BA networks get obviously more resilient than RANs. The critical thresholds of RANs and BA networks are $p_c^{RAN}\approx 0.85$ and $p_c^{BA}\approx 0.95$, which will approach 1 as the networks grow in size [91]. All the data are averaged over 100 independent simulations.

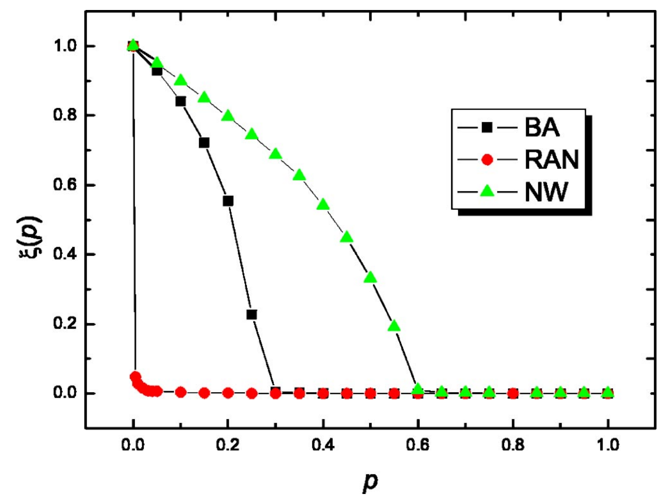

FIG. 8. (Color online) The preferential site-percolation for RANs (red circles) and BA (black squares) and NW (green triangles) networks (from left to right) with $N=10\,000$ and $\langle k\rangle=6$ fixed. Plotted is the fraction of nodes that remains in the giant component under intentional attack of a fraction p of all nodes, $\xi(p)$, as a function of p. The critical threshold of RANs and BA and NW networks are $p_c^{RAN}\approx 0.03$, $p_c^{BA}\approx 0.3$, and $p_c^{NW}\approx 0.65$, respectively. All the data are averaged over 100 independent simulations.

$$\sum_i i f_i = 2m. \tag{9}$$

Combining Eqs. (8) and (9) and considering that each face has at least three edges, we have

$$2m \geqslant 3\sum_i f_i = 3f. \tag{10}$$

Then, using Euler's formula, one can obtain that

$$m \leqslant 3n-6. \tag{11}$$

That is to say, the maximum number of edges for a planar network with order n is $3n-6$. Apparently, the random Apollonian network with order N has $3N-6$ edges on the beam, thus all the RANs are maximal planar networks.

VI. PERCOLATION AND EPIDEMIC SPREADING ON RANDOM APOLLONIAN NETWORKS

As we mentioned above, close to many real-life networks, random Apollonian networks are both scale free and small world. Therefore, it is worthwhile to investigate the processes taking place upon RANs and directly compare these results with just small-world (like WS and NW networks) and just scale-free networks (like BA networks). These comparisons may give us deep insight into the dynamic properties of networks.

In this section, we will exhibit some simulation results on two extensively studied dynamic models, **percolation** and **epidemic spreading process**. Since the WS networks may be unconnected, we will use NW networks as exemplifications of small-world networks.

A. Percolation

In the year 2000, Albert *et al.* raised the questions of random failures and intentional attack on networks [88]. Part of these questions can be equally considered as site-percolation or bond-percolation on networks [156,157]. In this subsection, upon RANs and BA and NW networks, we will investigate two kinds of site-percolation, **random site percolation** (RSP) and **preferential site percolation** (PSP), which correspond to random failures and intentional attack aiming at nodes, respectively.

When such networks are subject to random breakdowns, a fraction p of the nodes and their incident edges are removed randomly. Their integrity might be compromised: when p exceeds a certain threshold, $p>p_c$, the network disintegrates into smaller, disconnected fragments. Below that critical threshold, there still exists a connected cluster named the giant component that spans the entire system (its size is proportional to that of the entire system). In Fig. 7, we report the simulation results for RSP upon RANs and BA and NW networks. RANs and BA networks are obviously more resilient than NW networks under random failures that agrees with the well-known conclusion [88,91]. According to the results obtained by Cohen *et al.* [91], RANs and BA networks do not have nontrivial critical threshold $p_c<1$ in the limit of large network order $N\to\infty$. However, for finite network order and large p, RANs are frailer than BA networks.

Figure 8 shows the performances of RANs and BA and

NW networks under intentional attack, which means the removal of nodes is not random, but rather nodes with the greatest degree are targeted first. One can find that the scale-free networks are far more sensitive to sabotage of a small fraction of the nodes, leading support to the view of Albert and Cohen *et al.* [88,92]. Although we know the critical threshold for PSP upon scale-free networks will decay to zero as the increasing of network order as $\lim_{N\to\infty} p_c=0$, we are surprised by the notable difference between RANs and BA networks when N is relatively small. For very large N (as $N\sim 10^6$ or even larger), the performances of RANs and BA networks are almost the same with $p_c<0.03$ [92]. However, the susceptivity to order of RANs and BA networks are completely different. BA networks are very sensitive to network order; for $N=10\,000$, its critical threshold is about ten times than the asymptotic value. And RANs are almost impervious to the change of network order. Since many real-life networks are of order in the range 10^3 to 10^5, this finding may be valuable in practicability.

Why do RANs and BA networks display completely different susceptivity to order changing? Does it owe to the difference of clustering structure or hierarchical structure? This problem puzzles us much. To study the finite-size effect for PSP upon scale-free networks in detail and to use the network model with tunable clustering coefficient [108] may reveal some news, which will be considered in the future.

B. Epidemic spreading process

Recent studies on epidemic spreading in complex networks indicate a particular relevance in the case of networks characterized by various topologies that in many cases present us with new epidemic propagation scenarios such as the absence of any epidemic threshold below which the infection cannot initiate a major outbreak [100,101]. The new scenarios are of practical interest in computer virus diffusion and the spreading of diseases in heterogeneous populations. However, most previous studies have been focused on the stationary properties of endemic states or the final prevalence (i.e., the number of infected individuals) of epidemics. For the sake of protecting networks and finding optimal strategies for the deployment of immunization resources, it is of practical importance to study the dynamical evolution of the outbreaks, which has been far less investigated before. Barthélemy *et al.* reported both the analytic and numerical results of velocity of epidemic outbreaks in BA networks, which leaves us very short response time in the deployment of control measures [106]. We have studied the same process in weighted scale-free networks and demonstrated that the larger dispersion of weight results in slower spreading, which may be a good news for us [107]. In this subsection, we intend to study how the connectivity pattern (i.e., topological structure) affects the epidemic spreading process in the outbreaks. Numerical simulations about RANs and BA and NW networks are drawn, which may give us more comprehensive sight into the corresponding dynamic behavior.

In order to study the dynamical evolution of epidemic outbreaks, we shall focus on the susceptible-infected (SI) model in which individuals can be in two discrete states,

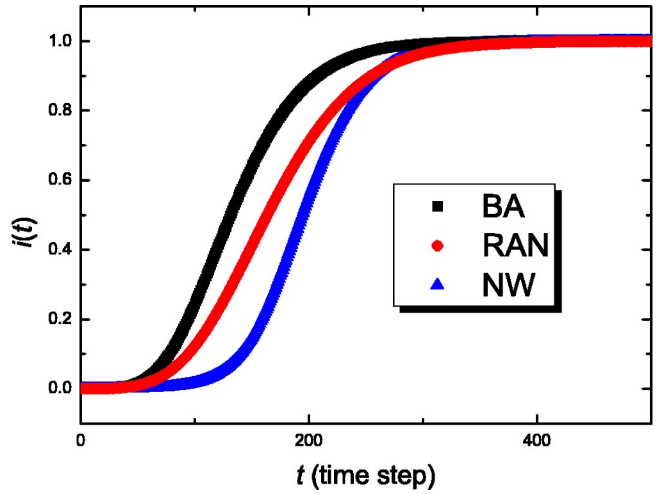

FIG. 9. (Color online) The average density of infected individuals versus time in networks with order $N=10\,000$ and average degree $\langle k\rangle=6$ fixed. The black, red, and blue curves (from top to bottom) correspond to the case of BA, RAN, and NW networks, respectively. The NW networks are of $z=1$ and $\phi=4\times10^{-4}$, thus $\langle k\rangle\approx 2z+\phi N=6$ [160] (see also the accurate definitions of z and ϕ in Ref. [83]). The spreading rate is $\lambda=0.01$. All the data are averaged over 10^3 independent runs.

either susceptible or infected [158,159]. Each individual is represented by a node of the network and the edges are the connections between individuals along which the infection may spread. The total population (the network order) N is assumed to be constant; thus if $S(t)$ and $I(t)$ are the number of susceptible and infected individuals at time t, respectively, then

$$N = S(t) + I(t). \qquad (12)$$

In the SI model, the infection transmission is defined by the spreading rate λ at which each susceptible individual acquires the infection from an infected neighbor during one time step. In this model, infected individuals are assumed to be always infective, which is an approximation that is useful to describe early epidemic stages in which no control measures are deployed. According to the definition, one can easily obtain the probability that a susceptible individual x will be infected at the present time step is

$$\lambda_x(t) = 1 - \lambda^{\theta(x,t-1)}, \qquad (13)$$

where $\theta(x,t-1)$ denotes the number of infected individuals at time step $t-1$ in x's neighbor set $A(x)$.

We start by selecting one node randomly and assume it is infected. The diseases or computer virus will spread on the networks in accord with Eqs. (13). In Fig. 9, we plot the average density over 1000 independent runs on RANs and BA and NW networks with $N=10\,000$ and $\langle k\rangle=6$ fixed. Obviously, all the individuals will be infected in the limit of long time as $\lim_{t\to\infty} i(t)=1$, where $i(t)=I(t)/N$ denotes the density of infected individuals at time step t. More over, the simulation results indicate that the diseases spread more quickly in BA networks than RANs, as well as in RANs than NW networks. To make the outcome more clear, we have

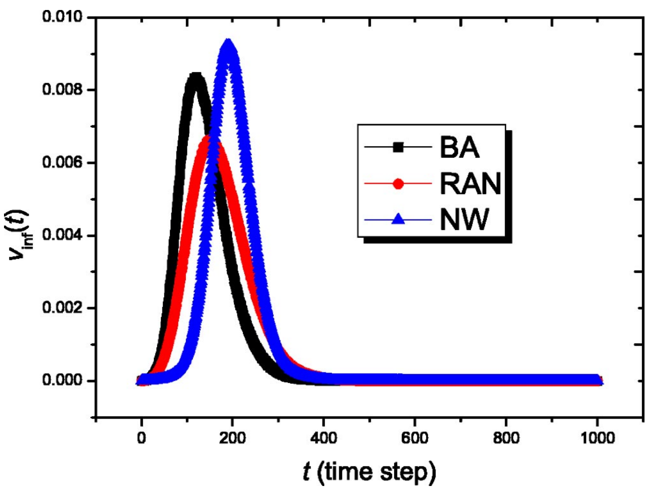

FIG. 10. (Color online) The spreading velocity versus time. The network order and spreading rate are the same with Fig. 9. The blue, red, and black curves (right to left) correspond to the cases of NW, RAN, and BA networks, respectively. The spreading velocity reaches a peak quickly. Before the peak time, the spreading velocities of the three kinds of networks satisfy the inequality $v_{inf}^{BA} > v_{inf}^{RAN} > v_{inf}^{NW}$. All the data are averaged over 10^3 independent runs.

calculated the diseases spreading velocity, which is defined as

$$v_{inf}(t) = \frac{di(t)}{dt} \approx \frac{I(t) - I(t-1)}{N}. \tag{14}$$

Figure 10 shows the spreading velocity versus time in RANs and BA and NW networks with $N=10\,000$ and $\langle k \rangle = 6$ fixed. The spreading velocity reaches a peak quickly. Before the peak time, the spreading velocities of the three kinds of networks satisfy the inequality

$$v_{inf}^{BA} > v_{inf}^{RAN} > v_{inf}^{NW}. \tag{15}$$

The result that diseases spread more quickly in RANs and BA networks than in NW networks is easy to be understood as the well-known conclusion: boarder degree distribution will speed up the epidemic spreading process [100,101].

Why the diseases spread more quickly in BA networks than RANs is a very interesting question. We argue that the larger clustering coefficient may slow down the epidemic spreading process, especially in the outbreaks. For an arbitrary edge e, containing two nodes x and y, obviously, the distance between x and y is $d(x,y)=1$. Remove the edge e from the quon-dam network, then, the distance between x and y will become $d'(x,y)>1$ [if the removal of e makes x and y disconnected, then we set $d'(x,y)=N$]. The quantity $d'(x,y)$ can be considered as edge e's score $s(e)=d'(x,y) \geqslant 2$, denoting the number of edges the diseases must pass through from x to y or form y to x if they do not pass across e. If $s(e)$ is small, then e only plays a local role in the epidemic spreading process, else when $s(e)$ is large, e is of global importance. For each edge e, if it makes some contribution to the clustering coefficient, it must be contained in at least one triangle and $s(e)=2$. Therefore, networks of larger clustering coefficient have more **local edges**. RANs and BA networks are two extreme ones of scale-free networks. In RANs, all the edges are of score 2, while in BA networks almost all the edges are of score larger than 2 because the clustering coefficient of BA networks will decay to zero quickly as N increases. Consequently, diseases spread more quickly in BA networks than RANs.

The above explanation is qualitative and rough; to study the process upon networks with tunable clustering coefficient [108] may be useful for the present problem, which will be one of the future works.

VII. CONCLUSIONS

In conclusion, in the respect that the random Apollonian networks are of very large clustering coefficient and very small average distance, they are not only the scale-free networks, but also small-world networks. Since most real-life networks are both scale-free and small-world, RANs may perform better in mimicking reality rather than BA and WS networks (or NW networks). In addition, RANs possess hierarchical structure in accord with the observations of many real networks and we propose an analytic approach to calculate clustering coefficient. Since the earlier studies only reported few analytic results about the clustering coefficient of networks with randomicity [149,153,161–163], we believe that our work may enlighten readers on this subject.

Furthermore, we briefly introduce the conception of planar network (it is also called "planar graph" in mathematical language), and prove that RANs are maximal planar networks, which are of particular practicability for layout of printed circuits and so on. Although whether a network is planar or not is a natural and important question that attracts much attention for mathematicians, it seems uninteresting for physicists and almost no pertinent results are reported in the earlier studies on complex networks. But, in fact, many real-life networks are planar networks by reason of technical or natural requirements, such as the layout of printed circuits, river networks upon the earth's surface, vas networks clinging to cutis, and so forth. Since the planar networks have some graceful characteristics that cannot be found in nonplanar ones, researchers ought to pay more attention to networks' planarity. We hope our abecedarian work could stimulate physicists to think more of planarity.

The percolation and epidemic spreading processes are also studies and the comparisons between RANs and BA as well as NW networks are shown. In the percolation model, we find that, when the network order N is relatively small (as $N \sim 10^4$), the performance of RANs under intentional attack is not sensitive to N, while that of BA networks is much affected by N. In the epidemic spreading process, the diseases spread slower in RANs than BA networks during the outbreaks, indicating that the large clustering coefficient may slow the spreading velocity, especially in the outbreaks. We give some qualitative explanation about how the clustering structure affects the spreading process in the outbreaks, but why RANs and BA networks display completely different susceptivity to order changing in the percolation process is even a problem puzzling us. Those simulation results suggest that the clustering structure may significantly affect the dynamical behavior upon networks. Since many real-life networks are of great clustering coefficient, to study the process upon networks with tunable clustering coefficient [108] is significant.

ACKNOWLEDGMENTS

The authors wish to thank Bo Hu for his help on preparing this manuscript. This work has been partially supported by the National Natural Science Foundation of China under Grants No. 70471033, 10472116, and 70271070, the Specialized Research Fund for the Doctoral Program of Higher Education (SRFDP No. 20020358009), and the Foundation for Graduate Students of University of Science and Technology of China under Grant No. KD200408.

APPENDIX A: MORE DETAILS FOR CALCULATION OF CLUSTERING COEFFICIENT

At first, let us consider the clustering coefficient $C(x)$ of an arbitrary node x except the nodes 1, 2, and 3. At the very time when node x is added to the network, it is of degree 3 and $E(x)\cdot=3$. After, if the degree of node x increases by 1 (i.e., a new node is added to be a neighbor of x) at some time step, then $E(x)$ will increase by 2 since the newly added node will link to two of the neighbors of node x. Therefore, we can write down the expression of $E(x)$ in terms of $k(x)$:

$$E(x) = 3 + 2[k(x) - 3] = 2k(x) - 3. \tag{A1}$$

Using Eq. (5), we can get the clustering coefficient of node x as

$$C(x) = \frac{2[2k(x) - 3]}{k(x)[k(x) - 1]}. \tag{A2}$$

Consequently, we have

$$C = \frac{2}{N}\sum_{i=1}^{N} \frac{2k_i - 3}{k_i(k_i - 1)} = \frac{2}{N}\sum_{i=1}^{N}\left(\frac{3}{k_i} - \frac{1}{k_i - 1}\right), \tag{A3}$$

where k_i denotes the degree of the ith node. Rewrite $\Sigma_{i=1}^{N} f(k_i)$ in continuous form:

$$\sum_{i=1}^{N} f(k_i) = \int_{k_{min}}^{k_{max}} Np(k)f(k)dk, \tag{A4}$$

where k_{min} and k_{max} denote the minimal and maximal degrees in RANs, respectively. Then, Eq. (A3) can be rewritten as

$$C = 6\int_{k_{min}}^{k_{max}} \frac{p(k)}{k}dk - 2\int_{k_{min}}^{k_{max}} \frac{p(k)}{k-1}dk. \tag{A5}$$

In Sec. IV, we have proved that $p(k)=\alpha k^{-\gamma}$ with $\gamma=3$ and α a constant, thus one can write down the expression that

$$C = 6\alpha\int_{k_{min}}^{k_{max}} k^{-4}dk - 2\alpha\int_{k_{min}}^{k_{max}} \frac{1}{k^3(k-1)}dk. \tag{A6}$$

Note that $1/k^3(k-1)=1/(k-1)-1/k-1/k^2-1/k^3$; one can immediately obtain the value of C as

$$C = 2\alpha\left(\frac{1}{k_{min}^3} + \frac{1}{2k_{min}^2} - \frac{1}{k_{min}} - \frac{1}{k_{max}} - \frac{1}{2k_{max}^2} - \frac{1}{k_{max}^3} - \ln\frac{k_{min}(k_{max}-1)}{k_{max}(k_{min}-1)}\right), \tag{A7}$$

It is clear that $k_{min}=3$ and for sufficiently large N, $k_{max} \gg k_{min}$, and α satisfies the normalization equation:

$$\int_{k_{min}}^{k_{max}} p(k)dk = 1. \tag{A8}$$

Therefore, $\alpha=18$ and $C=\frac{46}{3}-36\ln\frac{3}{2}\approx 0.74$.

APPENDIX B: THE AVERAGE DISTANCE

At first, let us prove an interesting property about the shortest paths in RANs. Mark each node according to the time when the node is added to the network (see Fig. 3). Then we have the following lemma:

Lemma: For any two nodes i and j, each shortest path from i to $j(SP_{ij})$ does not pass through any nodes k satisfying that $k>\max\{i,j\}$.

Proof: Use the nodes' sequence

$$i \to x_1 \to x_2 \to \cdots \to x_n \to j$$

to denote the shortest path from i to j of length $n+1$. Obviously, $n=0$ is the trivial case. Suppose that $n>0$ and $x_k=\max\{x_1,x_2,\ldots,x_n\}$, if $\forall 1\leqslant k\leqslant n, x_k<\max\{i,j\}$. Then the proposition is true.

In succession, we prove that the case $x_k>\max\{i,j\}$ would not come forth. Suppose that the triangle $\Delta y_1y_2y_3$ is selected when node x_k is added. Since $x_k>\max\{i,j\}$, neither i nor j is inside the triangle $\Delta y_1y_2y_3$. Hence the path from i to j passing through x_k must enter into and leave $\Delta y_1y_2y_3$. We may assume that the path enters into $\Delta y_1y_2y_3$ by node y_1 and leaves from node y_2. Then there exists a subpath of SP_{ij} from y_1 to y_2 passing through x_k, which is apparently longer than the direct path $y_1\to y_2$. Hence if SP_{ij} is the shortest path, the youngest node must be either i or j. ■

Using symbol $d(i,j)$ to represent the distance between i and j, the average distance of RANs with order N, denoted by $L(N)$, is defined as

$$L(N) = \frac{2\sigma(N)}{N(N-1)}, \tag{B1}$$

where the total distance is

$$\sigma(N) = \sum_{1\leqslant i<j\leqslant N} d(i,j). \tag{B2}$$

According to the lemma, the newly added node will not affect the distance between old nodes. Hence we have

$$\sigma(N+1) = \sigma(N) + \sum_{i=1}^{N} d(i,N+1). \tag{B3}$$

Assume that the node $N+1$ is added into the triangle $\Delta y_1y_2y_3$. Then Eq. (B3) can be rewritten as

$$\sigma(N+1) = \sigma(N) + \sum_{i=1}^{N} [D(i,y)+1] = \sigma(N) + N + \sum_{i=1}^{N} D(i,y), \tag{B4}$$

where $D(i,y)=\min\{d(i,y_1),d(i,y_2),d(i,y_3)\}$. Constrict $\Delta y_1y_2y_3$ continuously into a single node y. Then we have $D(i,y)=d(i,y)$. Since $d(y_1,y)=d(y_2,y)=d(y_3,y)=0$, Eq. (B4) can be rewritten as

$$\sigma(N+1) = \sigma(N) + N + \sum_{i\in\Gamma} d(i,y) \tag{B5}$$

where $\Gamma=\{1,2,\ldots,N\}-\{y_1,y_2,y_3\}$ is a node set with cardinality $N-3$.

The sum $\Sigma_{i\in\Gamma}d(i,y)$ can be considered as the total distance from one node y to all the other nodes in RANs with order $N-2$. The sum $\Sigma_{i\in\Gamma}d(i,y)$ is approximated in terms of $L(N-2)$:

$$\sum_{i\in\Gamma} d(i,y) \approx (N-3)L(N-2). \tag{B6}$$

Note that the average distance $L(N)$ increases monotonously with N. It is clear that

$$(N-3)L(N-2) = \frac{2\sigma(N-2)}{n-2} < \frac{2\sigma(N)}{N}. \tag{B7}$$

Combining (B5)–(B7), one can obtain the inequality

$$\sigma(N+1) < \sigma(N) + N + \frac{2\sigma(N)}{N}. \tag{B8}$$

If (B8) is not an inequality but an equation, then the increasing tendency of $\sigma(N)$ is determined by the equation

$$\frac{d\sigma(N)}{dN} = N + \frac{2\sigma(N)}{N}. \tag{B9}$$

This equation leads to

$$\sigma(N) = N^2 \ln N + H, \tag{B10}$$

where H is a constant. As $\sigma(N)\sim N^2L(N)$, we have $L(N)\sim \ln N$. Since Eq. (B8) is an inequality indeed, the precise increasing tendency of L may be a little slower than $\ln N$.

[1] R. Albert and A.-L. Barabási, Rev. Mod. Phys. **74**, 47 (2002).
[2] S. N. Dorogovtsev and J. F. F. Mendes, Adv. Phys. **51**, 1079 (2002).
[3] M. E. J. Newman, SIAM Rev. **45**, 167 (2003).
[4] M. E. J. Newman, J. Stat. Phys. **101**, 819 (2000).
[5] B. Hayes, Am. Sci. **88**, 9 (2000).
[6] B. Hayes, Am. Sci. **88**, 104 (2000).
[7] S. H. Strogatz, Nature (London) **410**, 268 (2001).
[8] X.-F. Wang, Int. J. Bifurcation Chaos Appl. Sci. Eng. **12**, 885 (2002).
[9] X.-F. Wang and G.-R. Chen, IEEE Circuits Syst. Mag. **3**, 6 (2003).
[10] T. S. Evans, arXiv: cond-mat/0405123.
[11] L. A. N. Amaral and J. M. Ottino, Eur. Phys. J. B **38**, 147 (2004).
[12] A.-L. Barabási, *Linked: The New Science of Networks* (Perseus, Cambridge, 2002).
[13] S. N. Dorogovtsev and J. F. F. Mendes, *Evolution of Networks: From Biological Nets to the Internet and WWW* (Oxford University Press, Oxford, 2003).
[14] D. J. Watts, *Small Worlds* (Princeton University Press, Princeton, 1999).
[15] M. Faloutsos, P. Faloutsos, and C. Faloutsos, Comput. Commun. Rev. **29**, 251 (1999).
[16] R. Pastor-Satorras, A. Vázquez, and A. Vespignani, Phys. Rev. Lett. **87**, 258701 (2001).
[17] G. Caldarell, R. Marchetti, and L. Pietronero, Europhys. Lett. **52**, 386 (2000).
[18] B. A. Huberman, *The Laws of the Web* (MIT, Cambridge, 2001).
[19] A.-L. Barabási, R. Albert, and H. Jeong, Physica A **281**, 69 (2000).
[20] G. W. Flake, S. R. Lawerence, C. L. Giles, and F. M. Coetzee, IEEE Comput. **35**, 66 (2002).
[21] A. Broder, R. Kumar, F. Maghoul., P. Raghavan, S. Rajagopalan, R. Stata, A. Tomkins, and J. Wener, Comput. Netw. **33**, 309 (2000).
[22] R. Albert, H. Jeong, and A.-L. Barabási, Nature (London) **401**, 130 (1999).
[23] J. Scott, *Social Network Analysis: A Handbook* (Sage Publications, London, 2000).
[24] S. Wasserman and K. Faust, *Social Network Analysis* (Cambridge University Press, Cambridge, 1994).
[25] F. Liljeros, C. R. Edling, L. A. N. Amaral, H. E. Stanley, and Y. Åberg, Nature (London) **411**, 907 (2001).
[26] J. J. Potterat, L. Phillips-Plummer, S. Q. Muth, R. B. Rothenberg, D. E. Woodhouse, T. S. Maldonado-Long, H. P. Zimmerman, and J. B. Muth, Sex Transm. Infect. **78**, i159 (2002).
[27] M. Morris, AIDS 97: Year Rev. **11**, 209 (1997).
[28] M. E. J. Newman, Phys. Rev. E **64**, 016131 (2004).
[29] M. E. J. Newman, Phys. Rev. E **64**, 016132 (2004).
[30] Y. Fan, M. Li, J. Chen, L. Gao, Z. Di, and J. Wu, Int. J. Mod. Phys. B **18**, 2505 (2004).
[31] M. Li, Y. Fan, J. Chen, L. Gao, Z. Di, and J. Wu, arXiv: cond-mat/0409272 Physica A (to be published).
[32] M. Li, J. Wu, D. Wang, T. Zhou, Z. Di, and Y. Fan, arXiv: cond-mat/0501655.
[33] B. Hu, X.-Y. Jiang, J.-F. Ding, Y.-B. Xie, and B.-H. Wang, arXiv: cond-mat/0408125.
[34] B. Hu, X.-Y. Jiang, B.-H. Wang, J.-F. Ding, T. Zhou, and Y.-B. Xie, arXiv: cond-mat/0408126.
[35] H. Jeong, B. Tombor, R. Albert, Z. N. Oltvai, and A.-L. Barabási, Nature (London) **407**, 651 (2000).
[36] J. Padani, Z. N. Oltvai, B. Tombor, A.-L. Barabási, and E.

Szathmary, Nat. Genet. **29**, 54 (2001).
[37] D. A. Fell and A. Wagner, Nat. Biotechnol. **18**, 1121 (2000).
[38] A. Wagner and D. A. Fell, Proc. R. Soc. London, Ser. B **268**, 1803 (2001).
[39] J. Stelling, S. Klamt, K. Bettenbrock, S. Schuster, and E. D. Gilles, Nature (London) **420**, 190 (2002).
[40] S. L. Pimm, *Food Webs* (University of Chicago, Chicago, 2002).
[41] J. M. Montoya and R. V. Solé, J. Theor. Biol. **214**, 405 (2002).
[42] R. V. Solé and J. M. Montoya, Proc. R. Soc. London, Ser. B **268**, 2039 (2001).
[43] J. Camacho, R. Guimerà, and L. A. Nunes Amaral, Phys. Rev. Lett. **88**, 228102 (2002).
[44] R. J. Williams, E. L. Berlow, J. A. Dunne, A.-L. Barabási, and N. D. Martinez, Proc. Natl. Acad. Sci. U.S.A. **99**, 12913 (2002).
[45] J. A. Dunne, R. J. Williams, and N. D. Martinez, Proc. Natl. Acad. Sci. U.S.A. **99**, 12917 (2002).
[46] J. A. Dunne, R. J. Williams, and N. D. Martinez, Ecol. Lett. **5**, 558 (2002).
[47] S. Redner, Eur. Phys. J. B **4**, 131 (1998).
[48] L. A. N. Amaral, A. Scala, M. Barthélémy, and H. E. Stanley, Proc. Natl. Acad. Sci. U.S.A. **97**, 11149 (2000).
[49] Y. He, X. Zhu, and D.-R. He, Int. J. Mod. Phys. B **18**, 2595 (2004).
[50] T. Xu, J. Chen, Y. He, and D.-R. He, Int. J. Mod. Phys. B **18**, 2599 (2004).
[51] V. Latora and M. Marchiori, Physica A **314**, 109 (2002).
[52] P. Sen, S. Dasgupta, A. Chatterjee, P. A. Sreeram, G. Mukherjee, and S. S. Manna, Phys. Rev. E **67**, 036106 (2003).
[53] A. Maritan, A. Rinaldo, R. Rigon, A. Giacometti, and I. Rodríguez-Iturbe, Phys. Rev. E **53**, 1510 (1996).
[54] R. Ferrer i Cancho, C. Janssen, and R. V. Solé, Phys. Rev. E **64**, 046119 (2001).
[55] O. Sporns, Complexity **8**(1), 56 (2002).
[56] J. R. Banavar, A. Maritan, and A. Rinaldo, Nature (London) **399**, 130 (1999).
[57] G. B. West, J. H. Brown, and B. J. Enquist, Science **276**, 122 (1997).
[58] G. B. West, J. H. Brown, and B. J. Enquist, Nature (London) **400**, 664 (1999).
[59] J.-M. Xu, *Topological Structure and Analysis of Interconnection Network* (Kluwer Academic, Dordrecht, 2001).
[60] J.-M. Xu, *Theory and Application of Graphs* (Kluwer Academic, Dordrecht, 2003).
[61] J. Bond and U. S. R. Murty, *Graph Theory with Applications* (MacMillan, London, 1976).
[62] B. Bollobás, *Modern Graph Theory* (Springer-Verlag, New York, 1998).
[63] P. Erdös, Bull. Am. Math. Soc. **53**, 292 (1947).
[64] R. Solomonoff and A. Rapoport, Bull. Math. Biophys. **13**, 107 (1951).
[65] P. Erdös and A. Rényi, Publ. Math. (Debrecen) **6**, 290 (1959).
[66] P. Erdös and A. Rényi, Publ. Math. Inst. Hung. Acad. Sci. **5**, 17 (1960).
[67] P. Erdös and A. Rényi, Acta Math. Acad. Sci. Hung. **12**, 261 (1961).
[68] M. Karonski, J. Graph Theory **6**, 349 (1982).
[69] B. Bollobás, *Random Graphs* (Academic, London, 1985).
[70] S. Janson, T. Łuczak, and A. Rucinski, *Random Graphs* (Wiley, New York, 1999).
[71] S. Milgram, Psychol. Today **2**, 60 (1967).
[72] D. J. Watts and S. H. Strogatz, Nature (London) **393**, 440 (1998).
[73] D. J. Watts, Am. J. Sociol. **105**, 493 (1999).
[74] M. E. J. Newman and D. J. Watts, Phys. Lett. A **263**, 341 (1999).
[75] R. Monasson, Eur. Phys. J. B **12**, 555 (1999).
[76] C.-P. Zhu, S.-J. Xiong, Y.-J. Tian, N. Li, and K.-S. Jiang, Phys. Rev. Lett. **92**, 218702 (2004).
[77] A.-L. Barabási and R. Albert, Science **286**, 509 (1999).
[78] A.-L. Barabási, R. Albert, and H. Jeong, Physica A **272**, 173 (1999).
[79] D. J. de S. Price, Science **149**, 510 (1965).
[80] D. J. de S. Price, J. Am. Soc. Inf. Sci. **27**, 292 (1976).
[81] M. A. de Menezes, C. Moukarzel, and T. J. P. Penna, Europhys. Lett. **50**, 574 (2000).
[82] C. F. Moukarzel, Phys. Rev. E **60**, R6263 (1999).
[83] M. E. J. Newman and D. J. Watts, Phys. Rev. E **60**, 7332 (1999).
[84] M. Ozana, Europhys. Lett. **55**, 762 (2001).
[85] S. Jespersen and A. Blumen, Phys. Rev. E **62**, 6270 (2000).
[86] J. M. Kleinberg, Nature (London) **406**, 845 (2000).
[87] P. Sen and B. K. Chakrabarti, J. Phys. A **34**, 7749 (2001).
[88] R. Albert, H. Jeong, and A.-L. Barabási, Nature (London) **406**, 378 (2000).
[89] C. Moore and M. E. J. Newman, Phys. Rev. E **62** 7059 (2000).
[90] D. S. Callaway, M. E. J. Newman, S. H. Strogatz, and D. J. Watts, Phys. Rev. Lett. **85**, 5468 (2000).
[91] R. Cohen, K. Erez, D. ben-Avraham, and S. Havlin, Phys. Rev. Lett. **85**, 4626 (2000).
[92] R. Cohen, K. Erez, D. ben-Avraham, and S. Havlin, Phys. Rev. Lett. **86**, 3682 (2001).
[93] S. N. Dorogovtsev and J. F. F. Mendes, Phys. Rev. Lett. **87**, 219801 (2001).
[94] N. Schwartz, R. Cohen, D. ben-Avraham, A.-L. Barabási, and S. Havlin, Phys. Rev. E **66**, 015104 (2002).
[95] N. Sarshar, P. O. Boykin, and V. P. Roychowdhury, arXiv: cond-mat/0406152.
[96] F. Jasch, C. von Ferber, and A. Blumen, Phys. Rev. E **70**, 016112 (2004).
[97] G. Palla, I. Derenyi, I. Farkas, and T. Vicsek, Phys. Rev. E **69**, 046117 (2004).
[98] S. N. Dorogovtsev, Phys. Rev. E **67**, 045102 (2003).
[99] S. N. Dorogovtsev, A. V. Goltsev, and J. F. F. Mendes, Eur. Phys. J. B **38**, 177 (2004).
[100] R. Pastor-Satorras and A. Vespignani, Phys. Rev. Lett. **86**, 3200 (2001).
[101] R. Pastor-Satorras and A. Vespignani, Phys. Rev. E **63**, 066117 (2001).
[102] M. Boguna and R. Pastor-Satorras, Phys. Rev. E **66**, 047104 (2002).
[103] M. Boguna, R. Pastor-Satorras, and A. Vespignani, Phys. Rev. Lett. **90**, 028701 (2003).
[104] R. M. May and A. L. Lloyd, Phys. Rev. E **64**, 066112 (2001).
[105] R. Pastor-Satorras and A. Vespignani, Phys. Rev. E **65**, 035108 (2002).
[106] M. Barthélemy, A. Barrat, R. Pastor-Satorras, and A. Vespignani, Phys. Rev. Lett. **92**, 178701 (2004).
[107] G. Yan, T. Zhou, J. Wang, Z.-Q. Fu, and B.-H. Wang, Chin.

Phys. Lett. **22**, 510 (2005).
[108] P. Holme and B. J. Kim, Phys. Rev. E **65**, 066109 (2002).
[109] P. Holme, Phys. Rev. E **66**, 036119 (2002).
[110] Y. Moreno, J. B. Gómez, and A. F. Pacheco, Europhys. Lett. **58**, 630 (2002).
[111] Y. Moreno, R. Pastor-Satorras, A. Vázquez, and A. Vespignani, Europhys. Lett. **62**, 292 (2003).
[112] A. E. Motter and Y.-C. Lai, Phys. Rev. E **66**, 065102 (2002).
[113] A. E. Motter, Phys. Rev. Lett. **93**,098701 (2004).
[114] K.-I. Goh, D.-S. Lee, B. Kahng, and D. Kim, Phys. Rev. Lett. **91**, 148701 (2003).
[115] D.-S. Lee, K.-I. Goh, B. Kahng, and D. Kim, Physica A **338**, 84 (2004).
[116] T. Zhou and B.-H. Wang,Chin. Phys. Lett. **22**, 1072 (2005).
[117] H. A. Simon, Biometrika **42**, 425 (1955).
[118] S. Bornholdt and H. Ebel, Phys. Rev. E **64**, 035104 (2001).
[119] P. L. Krapivsky, S. Redner, and F. Leyvraz, Phys. Rev. Lett. **85**, 4629 (2000).
[120] P. L. Krapivsky and S. Redner, Phys. Rev. E **63**, 066123 (2001).
[121] S. N. Dorogovtsev, J. F. F. Mendes, and A. N. Samukhin, Phys. Rev. Lett. **85**, 4633 (2000).
[122] S. N. Dorogovtsev and J. F. F. Mendes, Europhys. Lett. **52**, 33 (2000).
[123] S. N. Dorogovtsev and J. F. F. Mendes, Phys. Rev. E **63**, 025101 (2001).
[124] R. Albert and A.-L. Barabási, Phys. Rev. Lett. **85**, 5234 (2000).
[125] B. Tadić, Physica A **293**, 273 (2001).
[126] B. Tadić, Physica A **314**, 278 (2002).
[127] G. Bianconi and A.-L. Barabási, Phys. Rev. Lett. **86**, 5632 (2001).
[128] G. Bianconi and A.-L. Barabási, Europhys. Lett. **54**, 436 (2001).
[129] B.-S. Yuan, K. Chen, and B.-H. Wang, arXiv: cond-mat/0408391.
[130] K. Deng and Y. Tang, Chin. Phys. Lett. **21**, 1858 (2004).
[131] C.-G. Li and G.-R. Chen, Physica A **343**, 288 (2004).
[132] A. Capocci, G. Caldarelli, R. Marchetti, and L. Pietronero, Phys. Rev. E **64**, 035105 (2001).
[133] J. Berg and M. Lässig, Phys. Rev. Lett. **89**, 228701 (2002).
[134] M. Baiesi and S. S. Manna, Phys. Rev. E **68**, 047103 (2003).
[135] B. J. Kim, A. Trusina, P. Minnhagen, and K. Sneppen, arXiv: nlin.A0/0403006.
[136] G. Yan, T. Zhou, Y.-D. Jin, and Z.-Q. Fu, arXiv: cond-mat/0408631.
[137] S. Jain and S. Krishna, Phys. Rev. Lett. **81**, 5684 (1998).
[138] S. Jain and S. Krishna, Proc. Natl. Acad. Sci. U.S.A. **98**, 543 (2001).
[139] R. V. Sóle, R. Pastor-Satorras, E. Smith, and T. B. Kepler, Adv. Complex Syst. **5**, 43 (2002).
[140] A. Vázquez, A. Flammini, A. Maritan, and A. Vespignani, ComPlexUs **1**, 38 (2003).
[141] A. Wagner, Mol. Biol. Evol. **18**, 1283 (2001).
[142] T. Zhou, B.-H. Wang, P.-Q. Jiang, Y.-B. Xie, and S.-L. Bu, arXiv: cond-mat/0405258.
[143] J. S. Andrade, Jr., H. J. Herrmann, R. F. S. Andrade, and L. R. da Silva, Phys. Rev. Lett. **94**, 018702 (2005).
[144] S. N. Dorogovtsev, J. F. F. Mendes, and A. N. Samukhin, Phys. Rev. E **63**, 062101 (2001).
[145] S. N. Dorogovtsev, A. V. Goltsev, and J. F. F. Mendes, Phys. Rev. E **65**, 066122 (2002).
[146] D. W. Boyd, Can. J. Math. **25**, 303 (1973).
[147] J. P. K. Doye and C. P. Massen, Phys. Rev. E **71**, 016128 (2005).
[148] In this paper, the terminology "order" means the number of nodes in network, which is also called network size in some other papers.
[149] K. Klemm and V. M. Eguíluz, Phys. Rev. E **65**, 036123 (2002).
[150] R. F. S. Andrade and H. J. Herrmann, arXiv: cond-mat/0411364.
[151] T. Zhou, G. Yan, P.-L. Zhou, Z.-Q. Fu, and B.-H. Wang, arXiv: cond-mat/0409414.
[152] The selected triangle is destroyed and replaced by three new triangles, thus the number of triangles increases by 2.
[153] E. Ravasz and A.-L. Barabási, Phys. Rev. E **67**, 026112 (2003).
[154] A. Trusina, S. Maslov, P. Minnhagen, and K. Sneppen, Phys. Rev. Lett. **92**, 178702 (2004).
[155] B.-J. Kim, Phys. Rev. Lett. **93**, 168701 (2004).
[156] P. Grassberger, Math. Biosci. **63**, 157 (1983).
[157] G. R. Grimmett, *Percolation* (Springer-Verlag, Berlin, 1989).
[158] R. M. Anderson and R. M. May, *Infectious Diseases in Humans* (Oxford University Press, Oxford, 1992).
[159] J. D. Murray, *Mathematical Biology* (Springer, New York, 1993).
[160] The symbols z and ϕ denote the average coordination number and the adding probability in generating NW networks, respectively.
[161] A. Barrat and M. Weigt, Eur. Phys. J. B **13**, 547 (2000).
[162] M. E. J. Newman, Comput. Phys. Commun. **147**, 40 (2002).
[163] G. Szabó, M. Alava, and J. Kertész, Phys. Rev. E **67**, 056102 (2003).